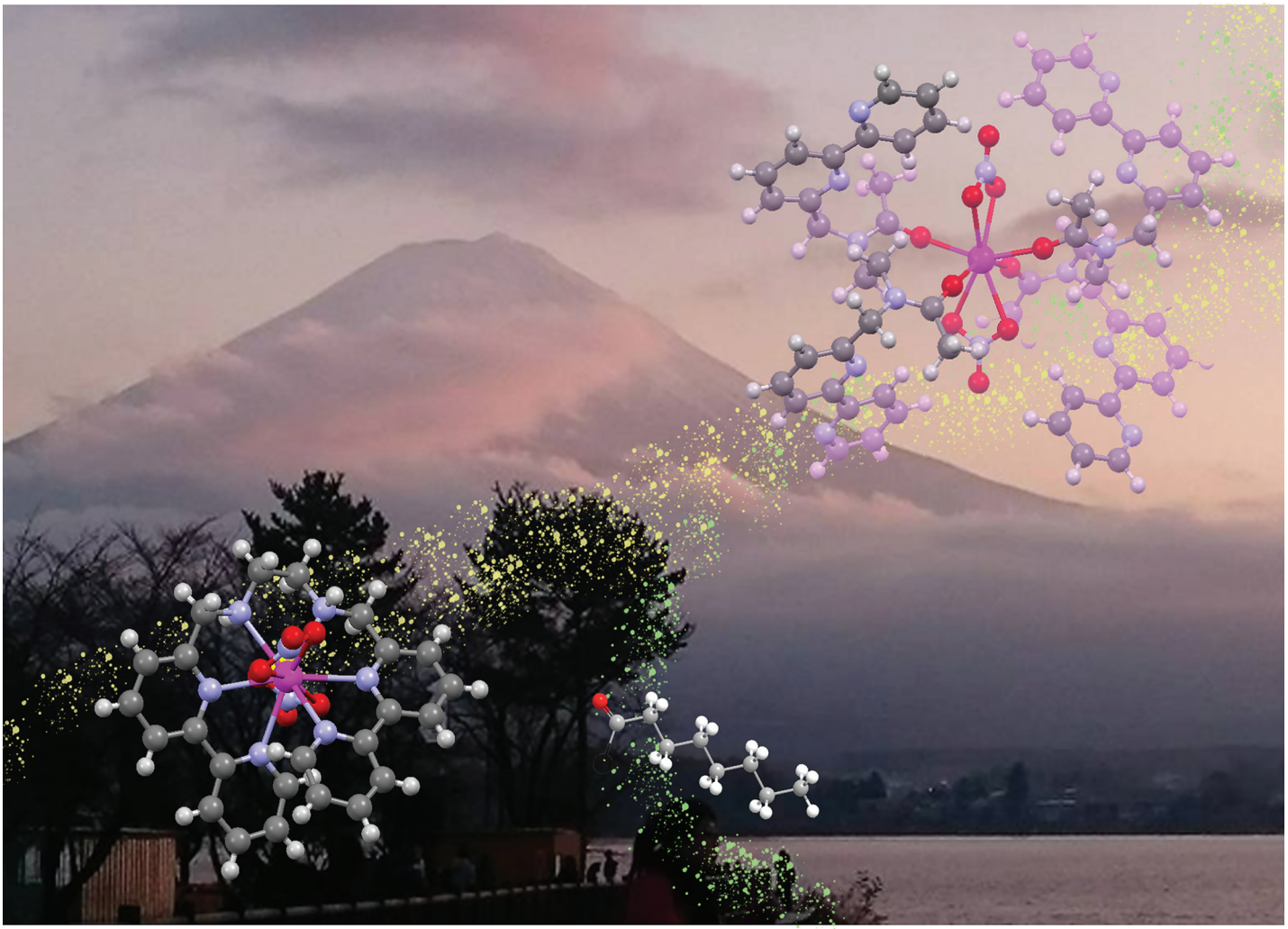

Showcasing research in collaboration of three groups; Miki Hasegawa (Aoyama Gakuin University), Miho Hatanaka (NAIST) and Kenta Goto (Kyushu University).

Alkyl chain elongation and acyl group effects in a series of Eu/Tb complexes with hexadentate π-electronic skeletons and their enhanced luminescence in solutions

Enhanced luminescence and structural aspects of bpy-based Eu complexes with various-length alkyl chains and acyl group was examined in solutions with theoretical evaluation. The metal/ligand 1:1 complexes transforms to the luminescent 1:2 complexes after alkyl-acylation.

As featured in:

See Miho Hatanaka, Miki Hasegawa *et al.*, *Dalton Trans.*, 2018, **47**, 7135.

ROYAL SOCIETY OF CHEMISTRY

rsc.li/dalton

Registered charity number: 207890

Dalton Transactions

PAPER

View Article Online
View Journal | View Issue

Check for updates

Cite this: *Dalton Trans.*, 2018, **47**, 7135

Alkyl chain elongation and acyl group effects in a series of Eu/Tb complexes with hexadentate π-electronic skeletons and their enhanced luminescence in solutions†

Shuhei Ogata,[a] Naoto Goto,[a] Shoya Sakurai,[a] Ayumi Ishii,[a,b] Miho Hatanaka,[*b,c] Koushi Yoshihara,[a] Ryota Tanabe,[a] Kyosuke Kayano,[a] Ryo Magaribuchi,[a] Kenta Goto[d] and Miki Hasegawa[*a]

Five Eu complexes with long alkyl chain groups, abbreviated as $EuLC_x$ ("*x*" indicates the number of methylene groups: *x* = 8, 12, 14, 18, and 22), were synthesized to evaluate their structural and luminescence properties in chloroform. The mother helicate Eu complex, EuL, which has two bipyridine moieties bridged by an ethylenediamine, has been previously reported. A reduced form in which the azomethine groups of L also coordinated to the Eu ion, EuLH, was newly prepared. EuLH also adopts a helicate molecular structure based on single crystal X-ray structural analysis. The amine hydrogens of the bridging ethylenediamine of LH are active sites for substitution and were exchanged with five different alkyl chains to form $EuLC_x$. Luminescence band positions and shapes of $EuLC_x$ in chloroform were completely identical, with a quantum yield of 37.1 ± 1.2 and a lifetime of around 1.25 ms. This indicates that the environments surrounding the Eu ion in the various complexes are all similar. Luminescence quantum yields of TbLH and $TbLC_{18}$ are also strengthened, 48.7% in acetonitrile and 55% in chloroform, respectively. Potential energy surfaces were also described by using density functional theory, suggesting the possibility of a 1 : 2 complex of Eu and the ligand as a main luminescent species in solutions. This 1 : 2 complexation forms Eu–oxygen coordination using acyl groups. It indicates that the acyl group modification results in a different structure from the mother complexes.

Received 27th December 2017,
Accepted 26th April 2018

DOI: 10.1039/c7dt04899h

rsc.li/dalton

Open Access Article. Published on 14 May 2018. Downloaded on 1/20/2026 1:24:30 PM.
This article is licensed under a Creative Commons Attribution-NonCommercial 3.0 Unported Licence.

1. Introduction

An advantage of lanthanide (Ln) complexes with π-electronic ligands is their stable luminescence colours originating from f–f transitions of Ln ions, which are strengthened by an antenna effect.[1,2] Based on this feature, luminescent Ln complexes have attracted much interest in applications for counterfeiting tags, devices, sensors, bioimaging and luminescent probes.[3–5]

Alkyl chain groups attached to a molecular structure can control not only the molecular size but also the chemical/physical properties such as hydrophilicity/hydrophobicity and solubility. It is well known that alkyl chain groups play an important role in biological systems.[6–8] For instance, phospholipids such as sphingomyelin and glycerophospholipid possess hydrophobic and hydrophilic moieties, and form phospholipid bilayers based on hydrophobic forces. The hydrophobic forces not only control the folding of proteins, but also help in maintaining their unique structures against deformation. Such a surfactant behaviour of the alkyl groups also has much potential in the fabrication of hybridized materials. In fact, we recently reported[9] a red-emissive graphene sheet hybridized with a Eu complex, $EuLC_{18}$, and studied its fundamental chemical properties.

Previously, we reported the mother complexes of Ln with helicate skeletons (LnL; Ln = Nd, Eu, Gd, Tb, Dy, and Ho).[10,11] The hexadentate ligand, L (Scheme 1), consists of two bipyridine (bpy) moieties bridged with an ethylenediamine. From single crystal X-ray structural analyses, all LnL complexes are

[a]*College of Science and Engineering, Aoyama Gakuin University, 5-10-1 Fuchinobe, Chuo-ku, Sagamihara, Kanagawa 252-5258, Japan.*
E-mail: hasemiki@chem.aoyama.ac.jp; Fax: +81-42-759-6221
[b]*JST, PRESTO, 4-1-8 Honcho, Kawaguchi, Saitama, 332-0012, Japan*
[c]*Institute for Research Initiatives, Division for Research Strategy, Graduate School of Materials Science, Data Science Center, Nara Institute for Science and Technology, 8916-5 Takayama-cho, Ikoma, Nara 630-0192, Japan.*
E-mail: hatanaka@ms.naist.ac.jp
[d]*Institute for Materials Chemistry and Engineering, Kyushu University, 744 Moto-oka, Fukuoka 819-0395, Japan*

†Electronic supplementary information (ESI) available: Packing structure with detailed structural information of EuLH, excitation spectra in solutions, calculation of rate constants for energy relaxation, luminescence decay profiles, and ^{1}H-NMR. CCDC 1813448. For ESI and crystallographic data in CIF or other electronic format see DOI: 10.1039/c7dt04899h

Open Access Article. Published on 14 May 2018. Downloaded on 1/20/2026 1:24:30 PM.
This article is licensed under a Creative Commons Attribution-NonCommercial 3.0 Unported Licence.

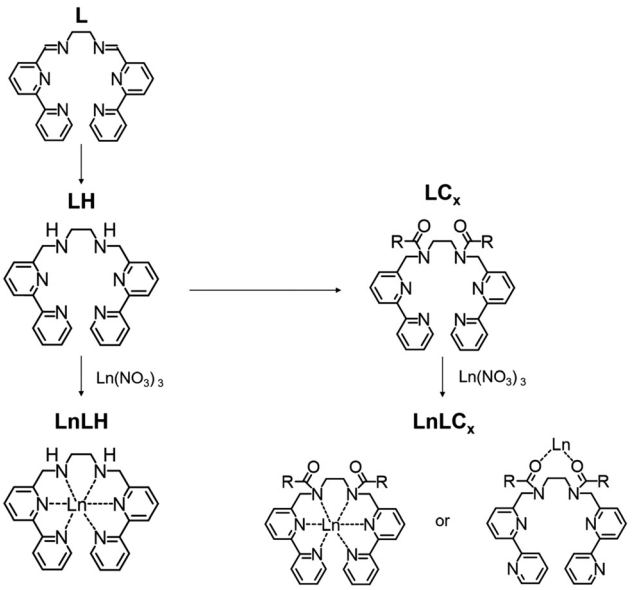

Scheme 1 Syntheses of $LnLC_x$ and LnLH. *R* and *x* indicate the alkyl group and its number of hydrocarbons, respectively.

isostructural. EuL in acetonitrile shows luminescence bands at 580, 595, 615, 650, and 685 nm by the irradiation of UV light. The luminescence and structural behaviours of LnL were stable even in acetonitrile due to the chelate effect. After the reduction of the azomethine moieties of LnL, derivatives that retained the luminescence were synthesized.[12] For instance, EuL^{COOH} shows high water solubility and luminescence with the same luminescence properties in the pH range of 2.6–9.7. The two carboxylic groups play different roles for the solubility and half-capsulation of the molecular form. We could also obtain EuL^{COOH}, which was derived from the reduced form of EuL. Here, a series of lanthanide complexes with various lengths of alkyl chains combined with LH (abbreviated as $EuLC_x$, x = 8, 12, 14, 18, and 22) were synthesized ($EuLC_8$, $EuLC_{12}$, $EuLC_{14}$, $EuLC_{18}$, and $EuLC_{22}$) and examined (Scheme 1). The mother molecule, EuLH, was also newly prepared in order to clarify the effect of the alkyl chain groups. Each ligand acts as a photo-antenna to sensitize the f–f emission localized on Eu^{III}. The electronic absorption spectra, luminescence spectra, absolute quantum yields and lifetimes of EuLH, $EuLC_8$, $EuLC_{12}$, $EuLC_{14}$, $EuLC_{18}$, and $EuLC_{22}$ were examined to elucidate their luminescence behaviour. Furthermore, the luminescent species and its stoichiometry of the Eu complex with LC_2 as a model molecule were elucidated by using density functional theory (DFT) calculations supporting mass spectroscopy.

2 Results and discussion

2.1 Structural analyses of Eu complexes with LH and LC_8

2.1.1 Structural analysis of EuLH. The single crystal X-ray structural analysis of EuLH was performed, and the molecular

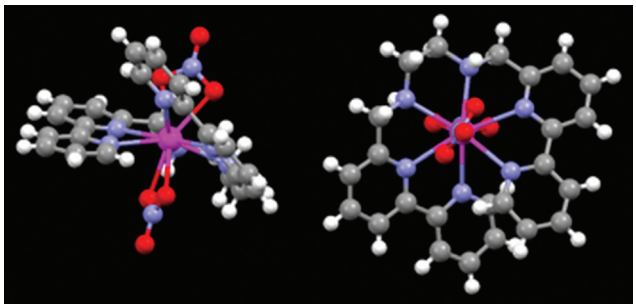

Fig. 1 Molecular structures of a couple of EuLH molecules determined from single crystal X-ray analysis. Coloured atoms in white, grey, blue, red, and pink indicate hydrogen, carbon, nitrogen, oxygen, and europium, respectively. NO_3 counter anions and acetonitrile atoms are omitted for clarity.

structure is shown in Fig. 1. Six nitrogen atoms of the ligand LH and four oxygen atoms of two nitrate ions coordinate to europium, and the complex adopts a 10-coordination structure. This complex also forms a helicate structure after the reduction of the azomethine moieties of EuL with the two nitrogen atoms of the ethylenediamine moieties. The C–N bond distance in EuLH of the reduced azomethine skeleton of EuL is 1.46 Å which is longer than the corresponding bond distance in EuL (1.27 Å). The bond angle of C(11)–N(3)–C(12) in EuLH (inset of Table S1†) is 112.8°, which corresponds to the value *ca.* 110° of H–C–H in methane with a sp^3-hybridized orbital. The averaged interatomic distance between europium and nitrogen atoms is *ca.* 2.49 Å with the longest and shortest ones being 2.61 and 2.53 Å, respectively.

Each bpy skeleton is planar and the distance between the two nearest carbon atoms located on the pyridine edges is *ca.* 3.28 Å. This value is higher than that of EuL by 0.1 Å, suggesting that the structures of EuL and EuLH are slightly different due to the azomethine reduction.

The *Z*-value of the unit cell was 4 (Table 1 and Fig. S1†), indicating that a couple of different structures of EuLH exist within the cell. Furthermore, four nitrate ions as counterions and six acetonitrile molecules are included in the unit cell. From the above results, there is enough space at the hydrogen atoms of azomethine's nitrogen to add alkyl chains due to the sp^3 hybridization of nitrogen atoms, as described above.

2.1.2 Coordination of Eu and LC_8 in solutions. From the ESI-MS measurement of $EuLC_8$ in acetonitrile (Fig. S2†), two main peaks appear at m/z = 924.87 and m/z = 1574.76. The former peak is assigned to $EuLC_8$ as a 1 : 1 stoichiometry of Eu and the ligand. The latter one corresponds to a 1 : 2 stoichiometric species of Eu and LC_8. As described later, the electronic absorption band and luminescence properties of the Eu complex with LC_8 differ from those of EuLH in solutions. Especially, there is only single component of the Eu complex with LC_8 in the luminescence lifetime. Thus, the stoichiometry or coordination sphere of Eu complexes with LC_x in solutions should be defined.

According to the DFT calculations, the Gibbs free energy of the model 1 : 2 complex $Eu(LC_2)_2(NO_3)_2$ was about 60 kcal mol^{-1}

This journal is © The Royal Society of Chemistry 2018

Open Access Article. Published on 14 May 2018. Downloaded on 1/20/2026 1:24:30 PM.
This article is licensed under a Creative Commons Attribution-NonCommercial 3.0 Unported Licence.

Table 1 Crystallographic data for EuLH

Formula	$C_{27}H_{28.5}EuN_{10.5}O_9$
Formula weight	796.05
Crystal size (mm)	0.137 × 0.162 × 0.063
Crystal system	Triclinic
Space group	$P\bar{1}$
a (Å)	11.3057(4)
b (Å)	15.635(2)
c (Å)	19.340(2)
α (°)	106.1440(10)
β (°)	91.3930(10)
γ (°)	105.6950(10)
V (Å^3)	3143.02
Z value	4
D_{calcd} (mg m^{-3})	1.682
μ (Mo Kα) (mm^{-1})	2.065
F(000)	1596
λ (Mo Kα) (Å)	0.71073
Temperature (K)	90
$R_1{}^a$ ($I > 2.00\sigma(I)$)	0.0309
$wR_2{}^b$ ($I > 2.00\sigma(I)$)	0.0677
Goodness of the fit	1.023
Largest peak and hole (e Å^{-3})	1.071, −0.609

$^a R_1 = \sum||F_o| - |F_c||/\sum|F_o|$. $^b wR_2 = \{\sum[w(F_o{}^2 - F_c{}^2)^2]/\sum[w(F_o{}^2)^2]\}^{1/2}$.

more stable than those of the model 1 : 1 complexes $EuLC_2(NO_3)_2$, which indicated that $EuLC_x$ could exist as 1 : 2 complexes. In the 1 : 2 complex, Eu was coordinated by two oxygen atoms of acyl groups instead of the nitrogen atoms of bpy moieties (Fig. 2).

2.2 Electronic absorption and luminescence of Eu complexes

2.2.1 EuLH in acetonitrile. The electronic absorption and luminescence spectra of EuLH, GdLH and the ligand LH are shown in Fig. 3. LH in acetonitrile mainly exhibits absorption bands at 286 and 300 (sh) nm. These bands shifted to a lower energy after complexation with Eu or Gd. EuLH has bands at 303 and 315 (sh) nm in acetonitrile. The band positions are at a higher energy than those of EuL,[10] meaning that the π-conjugated length decreased after the reduction of the azomethine moieties of the ligand.

The excited triplet level of the ligand, which is the key to sensitize the f–f emission, can be estimated from the phosphorescence bands of the Gd complexes (Fig. 3).[13–15] The phosphorescence band of GdLH in ethanol appears at 410 nm

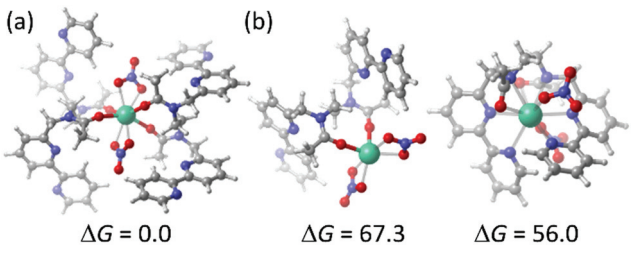

Fig. 2 Optimized geometries and Gibbs free energy differences at 298.15 K (in kcal mol^{-1}) of the 1 : 2 complex $Eu(LC_2)_2(NO_3)_2$ (a) and two 1 : 1 complexes $EuLC_2(NO_3)_2$ (b) calculated at the ωB97XD level of theory.

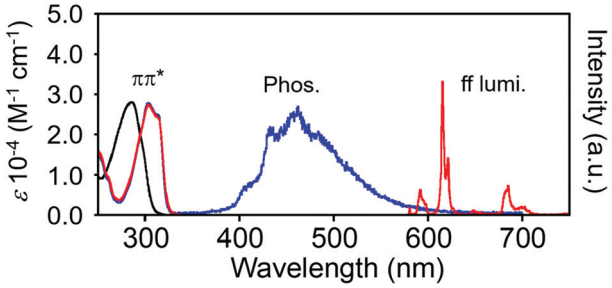

Fig. 3 Electronic absorption and luminescence spectra of EuLH (red) and GdLH (blue) in acetonitrile. The phosphorescence band was observed in ethanol at 77 K. The ligand is shown as a black line. λ_{ex} = 303 nm.

(24 400 cm^{-1}). The ligand LH acts as a sensitizer for Eu. The emission bands of EuLH were observed at 580.5, 592.3, 616.6, 649.7, and 686.2 nm in acetonitrile, assigned to the $^5D_0 \rightarrow {}^7F_0$, $^5D_0 \rightarrow {}^7F_1$, $^5D_0 \rightarrow {}^7F_2$, $^5D_0 \rightarrow {}^7F_3$, and $^5D_0 \rightarrow {}^7F_4$ transitions of Eu^{III}, respectively.

The excitation spectrum of EuLH corresponds to its absorption spectrum (Fig. S3†). The absolute luminescence quantum yield (ϕ_{L-Ln}) and luminescence lifetime (τ_{obs}) of EuLH in acetonitrile are 5.3% and 0.27 ms, respectively (Fig. S4†). The radiative rate constant (k_R), the non-radiative rate constant (k_{NR}), the efficiency of the metal centred luminescence (ϕ_{Ln-Ln}) and the efficiency of energy transfer from the triplet state of the ligand to Eu (η_{EnT}) are calculated from the equations shown in the ESI† using the above values. The values of k_R, k_{NR}, and η_{EnT} of EuLH are 267 (s^{-1}), 3437 (s^{-1}), and 74%, respectively. The value of k_{NR} is much higher than that of $EuLC_x$ as described later.

2.2.2 EuLCx in chloroform. The electronic absorption spectra of $EuLC_8$, $EuLC_{12}$, $EuLC_{14}$, $EuLC_{18}$, and $EuLC_{22}$ are shown in Fig. 4. After the modification of the ligand with two long alkyl chain groups, LC_8 shows an absorption band at nearly 290 nm in chloroform. The corresponding bands of

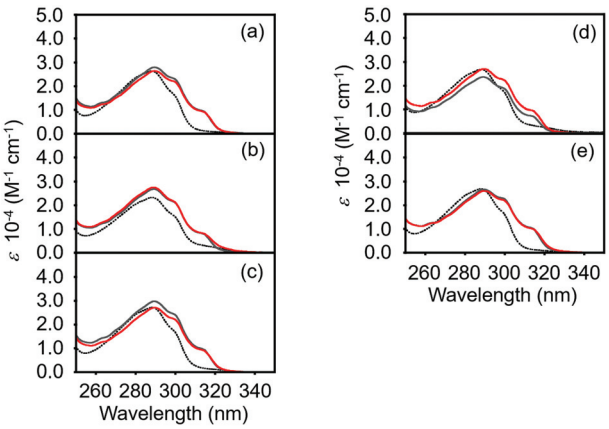

Fig. 4 Electronic absorption spectra of Eu (red line) and Gd (gray line) complexes with LC_8 (a), LC_{12} (b), LC_{14} (c), LC_{18} (d), and LC_{22} (e). Dotted lines correspond to free ligands.

Open Access Article. Published on 14 May 2018. Downloaded on 1/20/2026 1:24:30 PM.
This article is licensed under a Creative Commons Attribution-NonCommercial 3.0 Unported Licence.

$EuLC_8$ were observed at 290, 300 (sh), and 315 (sh) nm in chloroform. The spectral shapes of $EuLC_{12}$, $EuLC_{14}$, $EuLC_{18}$, and $EuLC_{22}$ in chloroform were identical to that of $EuLC_8$. This observation suggests that the long alkyl chain groups of the ligand moieties do not affect the electronic configuration surrounding the Eu ion and thus the series of $EuLC_x$ complexes adopt similar molecular structures in chloroform. The series of Gd complexes also shows corresponding bands in chloroform, while, these bands are different from that of EuLH in solutions.

The luminescence spectra of $EuLC_8$, $EuLC_{12}$, $EuLC_{14}$, $EuLC_{18}$, and $EuLC_{22}$ in chloroform are shown in Fig. 5. $EuLC_x$ also luminesces in the red wavelength region. $EuLC_8$ shows luminescence bands at 581.0, 592.5, 615.3, 649.8, and 685.0 nm in chloroform and these bands are assigned to the $^5D_0 \rightarrow {}^7F_0$, $^5D_0 \rightarrow {}^7F_1$, $^5D_0 \rightarrow {}^7F_2$, $^5D_0 \rightarrow {}^7F_3$, and $^5D_0 \rightarrow {}^7F_4$ transitions of Eu^{III}, respectively. The corresponding bands of $EuLC_{12}$, $EuLC_{14}$, $EuLC_{18}$, and $EuLC_{22}$ with different chain lengths appeared at the same positions. The spectral shapes of the series of $EuLC_x$ are completely identical indicating that the environment surrounding the Eu ion is similar for all the members of the series. Each excitation spectrum monitored at the f–f emission band positions reproduces well each electronic absorption spectrum assigned to the lowest excited state of LC_x (Fig. S5†).

To evaluate the energy donor level of each ligand as well as EuLH, Gd complexes with LC_x were used to determine the excited triplet state by the measurement of phosphorescence at a low temperature (Fig. 6). The band of $GdLC_{18}$ in solutions at 77 K appears around 425–600 nm as a broad band with some peaks and is slightly red-shifted more than that of GdLH. The band is reproduced well for other Gd complexes with LC_x, meaning that a series of different alkylation ligands LC_x can maintain the triplet state in their π-electronic systems. The fluorescence bands localized on the ligand of $GdLC_x$ at 332 nm in solutions reproduces that of GdLH which remains on the blue-side in GdL (Fig. S6†). $GdLC_x$ has a relatively clear shoulder around 360 nm. These results will maintain the possibility of a *quasi*-sp^2 conformation around the reduced azomethine moieties of the ligand LC_x after the complexation.

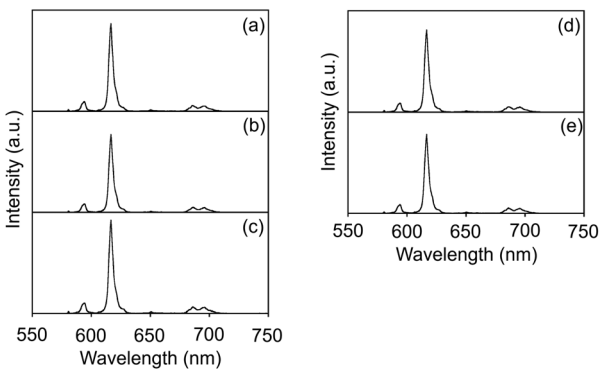

Fig. 5 Luminescence spectra of $EuLC_8$ (a), $EuLC_{12}$ (b), $EuLC_{14}$ (c), $EuLC_{18}$ (d), and $EuLC_{22}$ (e) in chloroform. λ_{ex} = 290 nm.

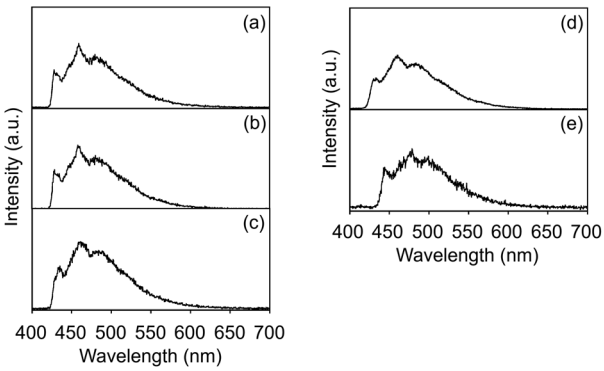

Fig. 6 Phosphorescence spectra of $GdLC_8$ (a), $GdLC_{12}$ (b), $GdLC_{14}$ (c), $GdLC_{18}$ (d), and $GdLC_{22}$ (e) in ethanol at 77 K. λ_{ex} = 290 nm.

The photophysical properties of $EuLC_8$, $EuLC_{12}$, $EuLC_{14}$, $EuLC_{18}$, and $EuLC_{22}$ are summarized in Table 2 and Fig. S7.† After the introduction of two long alkyl chain groups into the ligand, the values of ϕ_{L-Ln} were over 30% in a series of $EuLC_x$ which drastically changed compared with that in EuLH.

The τ_{obs} value of $EuLC_8$ is 1.24 ms as a single component and corresponds to those of $EuLC_{12}$, $EuLC_{14}$, $EuLC_{18}$, and $EuLC_{22}$ in chloroform. The value of k_{NR} drastically decreased after the introduction of alkyl chain groups. Thus, the two long alkyl chain groups are important to suppress the non-radiative relaxation process and sensitize the luminescence of the Eu ion. The k_R values of the series of $EuLC_x$ are similar, indicating that the environments around the Eu ion of $EuLC_x$ are the same. This is supported by spectral measurements. The η_{EnT} values of $EuLC_x$ are lower than that of EuLH. The molecular size-controlled Eu complexes with long alkyl chains were developed while maintaining the luminescence of the Eu ion.

The difference of luminescence properties between $EuLC_x$ and EuLH could be explained by the potential energy profiles (Fig. 7). The triplet energy levels of LC_2 and LH were similar because both of their excitations were localized on one of the bpy moieties.

From the triplet state, the energy transfer to Eu and quenching *via* the intersystem crossing could take place through the minimum energy crossing points between potential energy surfaces. The activation barrier for the quenching *via* the intersystem crossing between the triplet state and the

Table 2 Quantum yields (λ_{ex} = 300 nm), luminescence lifetimes (λ_{ex} = 280 nm and λ_{mon} = 618 nm) and photophysical data of $EuLC_8$, $EuLC_{12}$, $EuLC_{14}$, $EuLC_{18}$, $EuLC_{22}$, and EuLH

	φ_{L-Ln}	τ (ms)	k_R (s^{-1})	k_{NR} (s^{-1})	φ_{Ln-Ln}	η_{EnT}
$EuLC_8$	38.6%	1.24	539	261	67%	57%
$EuLC_{12}$	37.4%	1.25	539	261	67%	56%
$EuLC_{14}$	35.6%	1.25	543	257	68%	52%
$EuLC_{18}$	38.6%	1.25	538	262	68%	58%
$EuLC_{22}$	35.2%	1.25	543	258	68%	52%
EuLH	5.3%	0.27	267	3437	7%	74%

This journal is © The Royal Society of Chemistry 2018

Open Access Article. Published on 14 May 2018. Downloaded on 1/20/2026 1:24:30 PM.
This article is licensed under a Creative Commons Attribution-NonCommercial 3.0 Unported Licence.

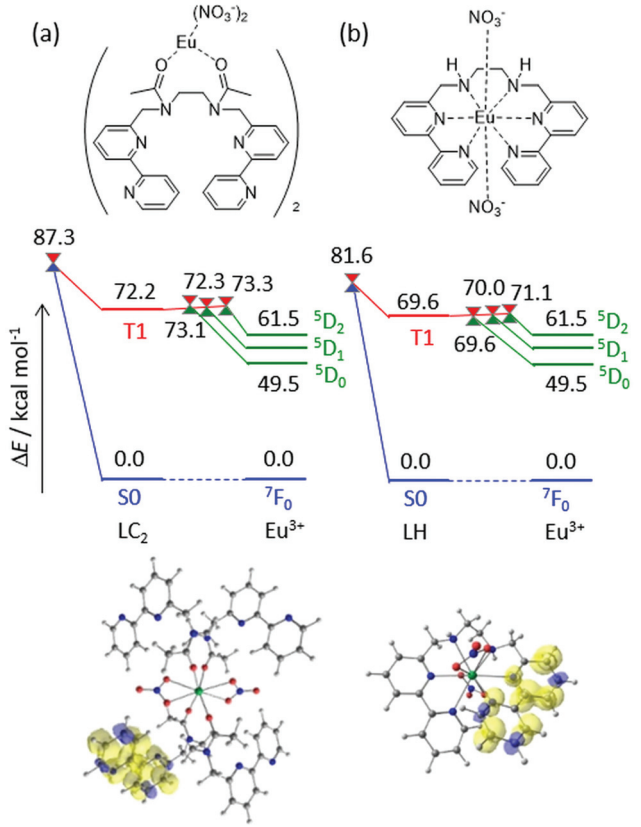

Fig. 7 Potential energy profiles (in kcal mol^{-1}) and spin densities on the ligand-centered triplet states of Eu(LC$_2$)$_2$(NO$_3$)$_2$ (a) and EuLH(NO$_3$)$_2$ (b) calculated using the DFT method with the ωB97XD functional. The double triangles represent the minimum energy crossing points between two potential energy surfaces.

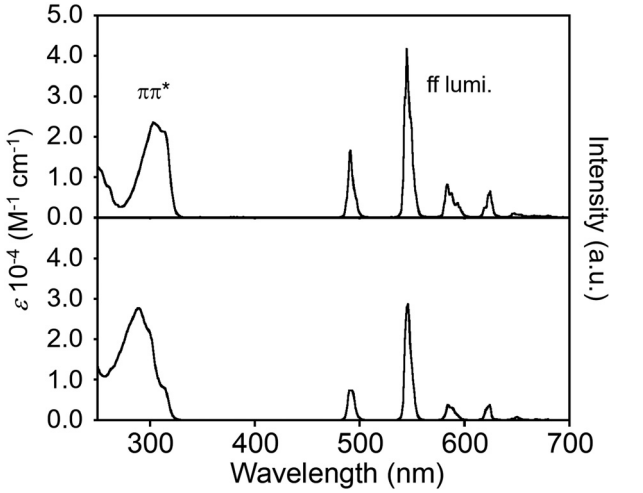

Fig. 8 Electronic absorption and luminescence spectra of TbLH (top: λ_{ex} = 305 nm) in acetonitrile and TbLC$_{18}$ (bottom: λ_{ex} = 290 nm) in chloroform.

ground state of EuLH was larger than that of EuLC$_2$, which resulted in a larger k_{NR} of EuLH. The activation barriers for the energy transfer were almost zero both for EuLC$_x$ and EuLH. However, the rate of the energy transfer for EuLC$_x$ could be slower than that of EuLH because the distance between Eu and excited bpy moieties in EuLC$_2$ was longer than that in EuLH,[16] which is consistent with a smaller η_{EnT} of EuLC$_x$.

2.3 Luminescence properties of TbLH in acetonitrile and TbLC$_{18}$ in chloroform

As reported previously, Eu and Tb complexes with the mother ligand L adopt the same molecular shape in the helicate form and luminesce from the center metals by UV excitation. To explore the possibilities of other Ln metals, we synthesized a Tb complex with LC$_{18}$ as a white powder (see the Experimental section).

The electronic absorption and luminescence spectra of TbLH and TbLC$_{18}$ in chloroform are shown in Fig. 8. The π–π* absorption bands of TbLH in acetonitrile appear at the corresponding positions of EuLH. TbLC$_{18}$ shows absorption bands at 290, 300 (sh) and 315 (sh) nm assigned to the π–π* transition. The absorption band position of TbLC$_{18}$ appeared at a shorter wavelength than that of TbL,[10] indicating that the electronic state of the ligand changed after the reduction of the azomethine moieties and the introduction of the alkyl chain groups.

We recently suggested that the reduction of L to LH will theoretically enhance the strong luminescence of the terbium ion.[17] Consequently, we experimentally realized the strong f–f emission of TbLH in acetonitrile. Thus, the band positions at 491.0, 545.0, 583.5, 624.5, and 647.5 nm are assigned to the $^5D_4 \rightarrow {}^7F_6$, $^5D_4 \rightarrow {}^7F_5$, $^5D_4 \rightarrow {}^7F_4$, $^5D_4 \rightarrow {}^7F_3$, and $^5D_4 \rightarrow {}^7F_2$ transitions of Tb^{III}, respectively, and the luminescence quantum yield becomes 48.7%, which is much higher than that of TbL (<0.1%) in acetonitrile.[10] In the case of TbL, the lowest minimum energy crossing from T_1 to S_0 is only 0.4 kcal mol^{-1} and the relaxation from the T_1 to S_0 occurs preferentially to transfer energy from the T_1 to $^5D_4$ resulting in a low quantum yield. In contrast, the energy level of the T_1 state of TbLH becomes higher than that of TbL as mentioned above (section 2.2.1). The energy barrier between the T_1 and S_0 also becomes higher. Thus, the absolute quantum yield in TbLH remarkably increased with the comparison of that in TbL. The luminescence decay curve demonstrates a single component with a lifetime of 1.66 ms (Fig. S8(a)†).

The luminescence bands of TbLC$_{18}$ in chloroform observed at 492.3, 547.2, 584.1, 625.9, and 650.1 nm are assigned to the $^5D_4 \rightarrow {}^7F_6$, $^5D_4 \rightarrow {}^7F_5$, $^5D_4 \rightarrow {}^7F_4$, $^5D_4 \rightarrow {}^7F_3$, and $^5D_4 \rightarrow {}^7F_2$ transitions of Tb^{III}, respectively. The mother molecule TbL shows negligibly weak luminescence in acetonitrile,[10] whereas the absolute luminescence quantum yield of TbLC$_{18}$ in chloroform is 55%, which is significantly higher than that of TbLH. The luminescence lifetime of this compound is 1.48 ms (Fig. S8(b)†). Thus, the reduction of the azomethine moieties and the introduction of the alkyl chain groups clearly affect the luminescence properties of Tb^{III} in solutions. The alkylation of the ligand in the Tb complex such as TbLC$_{18}$ results in more efficient luminescence than those in EuLC$_{18}$. It was

Open Access Article. Published on 14 May 2018. Downloaded on 1/20/2026 1:24:30 PM.
This article is licensed under a Creative Commons Attribution-NonCommercial 3.0 Unported Licence.

caused by a higher energy donor level of the ligand LC_{18} positioning at the acceptor level of Tb^{III} compared with the mother molecule L.

3. Experimental

3.1 Reagents and materials

Commercially available reagents and spectral-grade solvents (Wako Pure Chemical Industries Ltd, Tokyo Chemical Industry Ltd, and Kanto Chemical Co. Inc.) were generally used without further purification.

^{1}H-NMR spectra were recorded on a JEOL JMN-500 II spectrometer in $CDCl_3$ with tetramethylsilane. The X-ray structural data for EuLH were collected on a Bruker Smart APEX-II CCD diffractometer equipped with graphite monochromated Mo Kα radiation at 90 K. The data were collected to a maximum 2 h value of 55° and processed using the Bruker APEX-II software package.[18] The structure was solved by direct methods and refined by full-matrix least-squares calculations using a SHELX-97.[19–21] All non-hydrogen atoms were refined anisotropically, and all hydrogen atoms were located at the idealized positions. A summary of the fundamental crystal data and experimental parameters used to determine the structure of EuLH is given in the ESI.† CCDC 1813448.† Fast Atomic Bombardment (FAB-MS) was performed using the MStation JMS-700A (JEOL). Electron spray ionization mass spectroscopy (ESI-MS) was carried out by using JMS-T100CS (JEOL) and LCMS-8040 (Shimadzu) for $EuLC_8$ in acetonitrile and $EuLC_{18}$ and $TbLC_{18}$ in chloroform. Electronic absorption spectra were observed by using a UV-3600S (Shimadzu). Luminescence and excitation spectra were recorded on a Fluorolog 3–22 (Horiba Jobin Yvon). Absolute luminescence quantum yields and luminescence lifetimes were determined using an absolute luminescence quantum yield C9920-02 spectrometer (Hamamatsu Photonics K. K.) and a Quantaurus-Tau C11367-12 spectrometer (Hamamatsu Photonics K. K.), respectively, with pulsed excitation light sources.

3.2 Syntheses

3.2.1 EuLH and TbLH. The starting compound LH was synthesized using a previously reported method.[12] LH (100.0 mg, 252.2 μmol) and $Eu(NO_3)_3{\cdot}6H_2O$ (114.6 mg, 0.2570 μmol) were stirred in methanol (1 mL) for 3 hours. The precipitate was obtained after filtration. Yield: 115 mg (63%). MS (FAB^+); *m*/*z*, 673 $[M - (NO_3^-)]^+$ (calcd. 673.10).

TbLH was prepared similarly to EuLH using $Tb(NO_3)_3{\cdot}6H_2O$ (50.4 mg, 111.2 μmol). Yield: 58.1 mg (76%). MS (FAB^+); *m*/*z*, 679 $[M - (NO_3^-)]^+$ (calcd. 679.43).

3.2.2 *N*,*N*′-(Ethane-1,2-diyl)bis(*N*-([2,2′-bipyridin]-6-ylmethyl) octanamide) (LC_8). LH (181.9 mg, 458.8 μmol) was dissolved in tetrahydrofuran (10 mL) and *n*-octanoyl chloride (188.2 mg, 1157 μmol) in tetrahydrofuran (1 mL) was slowly added. Next, triethylamine (1553 mg, 15.36 mmol) in tetrahydrofuran (1 mL) was added to the mixture and the reaction mixture was stirred overnight. A white precipitate was filtered out and the filtrate was evaporated to dryness. The product was purified by column chromatography (chloroform/ethyl acetate, 7 : 3). Yield: 215.7 mg (72%). ^{1}H-NMR [500.00 MHz, $CDCl_3$, Fig. S9(a)†]: δ 8.66 (m, 2H), 8.30 (m, 4H), 7.75 (m, 4H), 7.29 (m, 4H), 4.78 (m, 4H), 3.70 (s, 4H), 2.38 (t, 4H), 1.60 (m, 4H), 1.25 (m, 16H), 0.88 (t, 6H). MS (FAB^+): *m*/*z* 648 $[M + H^+]^+$ (calcd. 648.42). Elemental analysis, calcd for $[LC_8]$ ($C_{40}H_{52}N_6O_2$): C 74.04, H 8.08, N 12.95; found: C 73.89, H 7.91, N 12.89.

3.2.3 *N*,*N*′-(Ethane-1,2-diyl)bis(*N*-([2,2′-bipyridin]-6-ylmethyl) dodecanamide) (LC_{12}). LH (182.5 mg, 460.3 μmol) was dissolved in tetrahydrofuran (10 mL) and *n*-lauroyl chloride (226.8 mg, 1037 μmol) in tetrahydrofuran (1 mL) was slowly added. Next, triethylamine (1000 mg, 9.882 mmol) in tetrahydrofuran (1 mL) was added to the mixture and the reaction mixture was stirred overnight. A white precipitate was filtered out and the filtrate was evaporated to dryness. The product was purified by column chromatography (chloroform/ethyl acetate, 6 : 4). Yield: 288.5 mg (82%). ^{1}H-NMR [500.00 MHz, $CDCl_3$, Fig. S9(b)†]: δ 8.67 (m, 2H), 8.31 (m, 4H), 7.75 (m, 4H), 7.30 (m, 4H), 4.78 (m, 4H), 3.71 (s, 4H), 2.41 (t, 4H), 1.64 (m, 4H), 1.21 (m, 32H), 0.87 (t, 6H). MS (FAB^+): *m*/*z* 760 $[M + H^+]^+$ (calcd. 760.54).

3.2.4 *N*,*N*′-(Ethane-1,2-diyl)bis(*N*-([2,2′-bipyridin]-6-ylmethyl) tetradecanamide) (LC_{14}). LH (124.2 mg, 152.0 μmol) was dissolved in tetrahydrofuran (10 mL) and *n*-myristoyl chloride (161.6 mg, 654.7 μmol) in tetrahydrofuran (1 mL) was slowly added. Next, triethylamine (912.2 mg, 9.014 mmol) in tetrahydrofuran (1 mL) was added to the mixture and the reaction mixture was stirred overnight. A white precipitate was filtered out and the filtrate was evaporated to dryness. The product was purified by column chromatography (chloroform/ethyl acetate, 6 : 4). Yield: 216.7 mg (80%). ^{1}H-NMR [500.00 MHz, $CDCl_3$, Fig. S9(c)†]: δ 8.66 (m, 2H), 8.32 (m, 4H), 7.79 (m, 4H), 7.30 (m, 4H), 4.78 (m, 4H), 3.70 (s, 4H), 2.38 (t, 4H), 1.62 (m, 4H), 1.24 (m, 40H), 0.87 (t, 6H). MS (FAB^+): *m*/*z* 816 $[M + H^+]^+$ (calcd. 816.60).

3.2.5 *N*,*N*′-(Ethane-1,2-diyl)bis(*N*-([2,2′-bipyridin]-6-ylmethyl) stearamide) (LC_{18}). LH (164.4 mg, 414.6 μmol) was dissolved in tetrahydrofuran (10 mL) and *n*-stearoyl chloride (276.9 mg, 914.1 μmol) in tetrahydrofuran (1 mL) was slowly added. Next, triethylamine (855.2 mg, 8.451 mmol) in tetrahydrofuran (1 mL) was added to the mixture and the reaction mixture was stirred overnight. A white precipitate was filtered out and the filtrate was evaporated to dryness. The product was purified by column chromatography (chloroform/ethyl acetate, 6 : 4). Yield: 253.5 mg (66%). ^{1}H-NMR [500.00 MHz, $CDCl_3$, Fig. S9(d)†]: δ 8.68 (m, 2H), 8.32 (m, 4H), 7.80 (m, 4H), 7.31 (m, 4H), 4.79 (m, 4H), 3.72 (s, 4H), 2.40 (t, 4H), 1.64 (m, 4H), 1.27 (d, 56H), 0.89 (t, 6H). MS (FAB^+): *m*/*z* 930 $[M + H^+]^+$ (calcd. 929.73).

3.2.6 *N*,*N*′-(Ethane-1,2-diyl)bis(*N*-([2,2′-bipyridin]-6-ylmethyl) behenamide) (LC_{22}). Docosanoic acid (398.1 mg, 1169 μmol) and thionyl chloride (6 mL) were stirred for 3 h at 333 K in toluene (10 mL) with a drop of *N*,*N*-dimethylformamide. *n*-Docosanoyl chloride was obtained after the evaporation of the mixture, which was used directly for the next reaction without further purification.

 This journal is © The Royal Society of Chemistry 2018

Open Access Article. Published on 14 May 2018. Downloaded on 1/20/2026 1:24:30 PM.
This article is licensed under a Creative Commons Attribution-NonCommercial 3.0 Unported Licence.

LH (166.2 mg, 419.1 μmol) was dissolved in tetrahydrofuran (10 mL) and *n*-docosanoyl chloride in tetrahydrofuran (2 mL) was slowly added. Next, triethylamine (1030 mg, 10.1 mmol) in tetrahydrofuran (1 mL) was added to the mixture and the reaction mixture was stirred overnight. A white precipitate was filtered out and the filtrate was evaporated to dryness. The product was purified by column chromatography (chloroform/ethyl acetate, 6 : 4). Yield: 346.3 mg (79%). ^{1}H-NMR (500.00 MHz, $CDCl_3$, Fig. S9(e)†): δ 8.66 (m, 2H), 8.31 (m, 4H), 7.79 (m, 4H), 7.30 (m, 4H), 4.78 (m, 4H), 3.70 (m, 4H), 2.39 (m, 4H), 1.62 (m, 4H), 1.26 (m, 72H), 0.88 (t, 6H). MS (FAB^+): *m*/*z* 1041 $[M + H]^+$ (calcd. 1040.85).

3.2.7 EuLC$_8$ and GdLC$_8$. LC_8 (148.5 mg, 228.8 μmol) was dispersed into hot ethanol (7 mL) and completely dissolved. After cooling the solution, $Eu(NO_3)_3{\cdot}6H_2O$ (131.8 mg, 295.5 μmol) in ethanol (1 mL) was slowly added to the solution and the reaction mixture was stirred for 30 minutes. A white precipitate was filtered and washed with cold ethanol. Yield: 156.8 mg (69%). FAB^+MS: *m*/*z* 925 $[M - (NO_3^-)]^+$ (calcd. 924.87). ESI-MS in acetonitrile: *m*/*z* 925.74 for $EuLC_8$ (calcd. 924.87) (Fig. S2(a)†) and *m*/*z* 1574.85 for $Eu(LC_8)_2$ (calcd. 1574.64) (Fig. S2(a)†) without each NO_3^- as a cation $[M - (NO_3^-)]^+$. Elemental analysis, calcd for $[EuLC_8]$ ($C_{40}H_{52}EuN_9O_{11}$): C 48.68, H 5.31, N 12.77; found: C 48.95, H 5.58, N 12.45.

$GdLC_8$ was prepared similarly to $EuLC_8$ using $Gd(NO_3)_3{\cdot}6H_2O$ (13.6 mg, 31.3 μmol). Yield: 21.3 mg (71%). MS (FAB^+): *m*/*z* 930 $[M - (NO_3^-)]^+$ (calcd. 930.15). Elemental analysis, calcd for $[GdLC_8]$ ($C_{40}H_{52}GdN_9O_{11}$): C 48.42, H 5.28, N 12.71; found: C 48.79, H 5.50, N 12.52.

3.2.8 EuLC$_{12}$ and GdLC$_{12}$. LC_{12} (154.8 mg, 189.4 μmol) was dispersed into hot ethanol (5 mL) and completely dissolved. After cooling the solution, $Eu(NO_3)_3{\cdot}6H_2O$ (106.1 mg, 237.9 μmol) in ethanol (0.5 mL) was slowly added to the solution and the reaction mixture was stirred for 30 minutes. A white precipitate was filtered and washed with cold ethanol. Yield: 158.5 mg (78%). MS (FAB^+): *m*/*z* 1037 $[M - (NO_3^-)]^+$ (calcd. 1037.08).

$GdLC_{12}$ was prepared similarly to $EuLC_{12}$ using $Gd(NO_3)_3{\cdot}6H_2O$ (47.4 mg, 105 μmol). Yield: 71.2 mg (67%). MS (FAB^+): *m*/*z* 1042 $[M - (NO_3^-)]^+$ (calcd. 1042.37).

3.2.9 EuLC$_{14}$ and GdLC$_{14}$. LC_{14} (154.8 mg, 189.4 μmol) was dispersed into hot ethanol (5 mL) and completely dissolved. After cooling the solution, $Eu(NO_3)_3{\cdot}6H_2O$ (101.4 mg, 227.3 μmol) in ethanol (0.5 mL) was slowly added to the solution and the reaction mixture was stirred for 30 minutes. A white precipitate was filtered and washed with cold ethanol. Yield: 157.8 mg (72%). MS (FAB^+): *m*/*z* 1093 $[M - (NO_3^-)]^+$ (calcd. 1093.19). Elemental analysis, calcd for $[EuLC_{14}]$ ($C_{52}H_{76}EuN_9O_{11}$): C 54.07, H 6.63, N 10.91; found: C 54.49, H 6.98, N 10.55.

$GdLC_{14}$ was prepared similarly to $EuLC_{14}$ using $Gd(NO_3)_3{\cdot}6H_2O$ (27.5 mg, 60.9 μmol). Yield: 38.3 g (98%). MS (FAB^+): *m*/*z* 1098 $[M - (NO_3^-)]^+$ (calcd. 1098.48). Elemental analysis, calcd for $[GdLC_{14}]$ ($C_{52}H_{76}GdN_9O_{11}$): C 54.20, H 6.86, N 10.61; found: C 53.82, H 6.60, N 10.86.

3.2.10 EuLC$_{18}$, GdLC$_{18}$ and TbLC$_{18}$. LC_{18} (141.2 mg, 151.9 μmol) was dispersed into hot ethanol (30 mL) and completely dissolved. After cooling the solution, $Eu(NO_3)_3{\cdot}6H_2O$ (79.47 mg, μmol) in ethanol (2 mL) was slowly added to the solution and the reaction mixture was stirred for 1 hour. A white precipitate was filtered and washed with cold ethanol. Yield: 141.5 mg (73%). MS (FAB^+): *m*/*z* 1205 $[M - (NO_3^-)]^+$ (calcd. 1205.62). ESI-MS in chloroform (Fig. S2(b)†): *m*/*z* 1205.6 $[M - (NO_3^-)]^+$ (calcd. 1205.62).

$GdLC_{18}$ was prepared similarly to $EuLC_{18}$ using $Gd(NO_3)_3{\cdot}6H_2O$ (19.2 mg, 42.7 μmol). Yield: 13.0 mg (25%). MS (FAB^+): *m*/*z* 1211 $[M - (NO_3^-)]^+$ (calcd. 1210.69).

$TbLC_{18}$ was also synthesized by using $Tb(NO_3)_3{\cdot}6H_2O$ (16.0 mg, 35.7 μmol). Yield: 10.0 mg (26%), MS (FAB^+): *m*/*z* 1212 $[M - (NO_3^-)]^+$ (calcd. 1211.63). ESI-MS in chloroform (Fig. S2(c)†): *m*/*z* 1211.7 $[M - (NO_3^-)]^+$ (calcd. 1211.63).

3.2.11 EuLC$_{22}$ and GdLC$_{22}$. LC_{22} (157.9 mg, 146.8 μmol) was dispersed into hot ethanol (10 mL) and completely dissolved. After cooling the solution, $Eu(NO_3)_3{\cdot}6H_2O$ (92.5 mg, 207.4 μmol) in ethanol (2 mL) was slowly added to the solution and the reaction was stirred for 1 hour. A white precipitate was filtered and washed with cold ethanol. Yield: 152.7 mg (75%). MS (FAB^+): *m*/*z* 1318 $[M - (NO_3^-)]^+$ (calcd. 1317.62).

$GdLC_{22}$ was prepared similarly to $EuLC_{22}$ using $Gd(NO_3)_3{\cdot}6H_2O$ (11.1 mg, 24.7 μmol). Yield: 25.7 mg (75%). MS (FAB^+): *m*/*z* 1323 $[M - (NO_3^-)]^+$ (calcd. 1322.91).

3.3 Computational

All the potential energy surfaces (PESs) were described using density functional theory (DFT) with the ωB97XD functional.[22] The basis sets for Eu^{3+} and others were the (7s6p5d)/[5s4p3d] Stuttgart-Dresden large-core RECP basis set[23] and cc-pVDZ,[24] respectively. The PESs of Eu^{3+}-centered excited states (^5D_J; J = 0, 1, and 2) were approximately represented by that of the ground state corrected by energy shift parameters[25] (17 250 cm^{-1}, 19 000 cm^{-1}, and 21 500 cm^{-1} for J = 0, 1, and 2, respectively). The details of this approximation, called the energy shift method, are shown in ref. 26 and 27. The geometry optimizations of local minima and minimum energy crossing points were performed *via* the global reaction route mapping (GRRM) program[28] using the energies and energy derivatives computed using the Gaussian09 program.[29]

4. Conclusions

Five europium complexes with long alkyl chain groups were successfully synthesized and their luminescence spectra were obtained quantitatively by means of luminescence lifetimes and quantum yields. Their periodical size change upon alkyl-derivatization on the π-electronic skeleton did not influence the luminescence of the resulting Eu complexes, $EuLC_x$, except for EuLH in solutions. Based on the DFT calculation concerned with the luminescence properties, it was found that the acyl groups of LC_x coordinate to Eu instead of bpy moieties in

Open Access Article. Published on 14 May 2018. Downloaded on 1/20/2026 1:24:30 PM.
This article is licensed under a Creative Commons Attribution-NonCommercial 3.0 Unported Licence.

solutions. Finally, it is known that the environments surrounding the Eu ion are similar to each other in solutions.

TbLH in acetonitrile shows enhanced luminescence based on the theoretical approaches in our previous report. The quantum yield of TbLH is quite high at 48.7% in comparison with the mother compound TbL. Furthermore, after the alkylation of TbLH to form $TbLC_{18}$, the f–f emission ability in solutions increases drastically.

Author contributions

M. Hasegawa conceived and designed the study with A. Ishii and K. Goto, S. Ogata, N. Goto, S. Sakurai, K. Yoshihara, R. Tanabe, K. Kayano, and R. Magaribuchi performed the experiments. M. Hatanaka provided the theoretical aspects to improve molecular designs.

Conflicts of interest

The authors declare no conflict of interest.

Acknowledgements

The authors acknowledge Prof. Makoto Handa and Prof. Michiko Egawa (Shimane University) for their kind discussions. This work was partly supported by grants-in-aid from Scientific Research on Innovative Areas of "Soft Crystals (area number: 2903)" (no. 17H06374; MH), MEXT Supported Program for the Strategic Research Foundation at Private Universities (2013–2017; MH), Network Joint Research Centre for Materials and Devices (2017; MH) and a SOKEN Project provided by Aoyama Gakuin University Research Institute (2016–2017; MH). MH also acknowledges Izumi Science and Technology Foundation for their financial support. SO thanks the Early Eagle Program for a subsidy from Aoyama Gakuin University. AI and Miho Hatanaka acknowledge the support of JST PRESTO.

Notes and references

1 S. I. Weissman, *J. Chem. Phys.*, 1942, **10**, 214.
2 S. Tobita, M. Arakawa and I. Tanaka, *J. Phys. Chem.*, 1985, **89**, 5649.
3 S. V. Eliseeva and J.-C. G. Bünzli, *Chem. Soc. Rev.*, 2010, **39**, 189.
4 X. Wang, H. Chang, J. Xie, B. Zhao, B. Liu, S. Xu, W. Pei, N. Ren, L. Huang and W. Huang, *Coord. Chem. Rev.*, 2014, **273–274**, 201.
5 H. Xu, C.-S. Cao, X.-M. Kanga and B. Zhao, *Dalton Trans.*, 2016, **45**, 18003.
6 C. Tanford, *Science*, 1978, **200**, 1012.
7 R. G. Snyder, H. L. Strauss and C. A. Elliger, *J. Phys. Chem.*, 1982, **86**, 5145.
8 H. R. Marsden, I. Tomatsu and A. Kros, *Chem. Soc. Rev.*, 2011, **40**, 1572.
9 Y. Hara, K. Yoshihara, K. Kondo, S. Ogata, T. Watanabe, A. Ishii, M. Hasegawa and S. Koh, *Appl. Phys. Lett.*, 2018, **112**, 173103.
10 M. Hasegawa, H. Ohtsu, D. Kodama, T. Kasai, S. Sakurai, A. Ishii and K. Suzuki, *New J. Chem.*, 2014, **38**, 1225.
11 H. Wada, S. Ooka, D. Iwasawa, M. Hasegawa and T. Kajiwara, *Magnetochemistry*, 2016, **2**, 43.
12 S. Ogata, T. Shimizu, T. Ishibashi, Y. Ishiyone, M. Hanami, M. Ito, A. Ishii, S. Kawaguchi, K. Sugimoto and M. Hasegawa, *New J. Chem.*, 2017, **41**, 6385.
13 G. H. Dieke and H. M. Crosswhite, *Appl. Opt.*, 1963, **2**, 675.
14 S. Comby, D. Imbert, A.-S. Chauvin and J.-C. G. Bünzli, *Inorg. Chem.*, 2006, **45**, 732.
15 C. Y. Chow, S. V. Eliseeva, E. R. Trivedi, T. N. Nguyen, J. W. Kampf, S. Petoud and V. L. Pecorato, *J. Am. Chem. Soc.*, 2016, **138**, 5100.
16 O. L. Malta, *J. Non-Cryst. Solids*, 2008, **354**, 4770.
17 M. Hatanaka, A. Osawa, T. Wakabayashi, K. Morokuma and M. Hasegawa, *Phys. Chem. Chem. Phys.*, 2018, **20**, 3328.
18 *SMART, SAINT, XPREP and SADABS*, Bruker AXS Inc., Madision, Wisconsin, 2004.
19 G. M. Sheldrick, *Acta Crystallogr., Sect. A: Fundam. Crystallogr.*, 2008, **64**, 112.
20 G. M. Sheldrick, *SHELXS-97*, University of Göttingen, Göttingen, 1997.
21 G. M. Sheldrick, *SHELX-97*, University of Göttingen, Göttingen, 1997.
22 J. D. Chai and M. Head-Gordon, *Phys. Chem. Chem. Phys.*, 2008, **10**, 6615.
23 M. Dolg, H. Stoll and H. Preuss, *Theor. Chim. Acta*, 1993, **85**, 441.
24 T. H. Dunning, *J. Chem. Phys.*, 1989, **90**, 1007.
25 K. Binnemans, *Coord. Chem. Rev.*, 2015, **295**, 1.
26 M. Hatanaka and K. Morokuma, *J. Chem. Theory Comput.*, 2014, **10**, 4184.
27 M. Hatanaka, Y. Hirai, Y. Kitagawa, T. Nakanishi, Y. Hasegawa and K. Morokuma, *Chem. Sci.*, 2017, **8**, 423.
28 S. Maeda, Y. Osada, T. Taketsugu, K. Morokuma and K. Ohno, *GRRM14*, http://iqce.jp/GRRM/index_e.shtml.
29 M. J. Frisch, G. W. Trucks, H. B. Schlegel, G. E. Scuseria, M. A. Robb, J. R. Cheeseman, J. A. Montgomery, T. Vreven, K. N. Kudin, J. C. Burant, J. M. Millam, S. S. Iyengar, J. Tomasi, V. Barone, B. Mennucci, M. Cossi, G. Scalmani, N. Rega, G. A. Petersson, H. Nakatsuji, M. Hada, M. Ehara, K. Toyota, R. Fukuda, J. Hasegawa, M. Ishida, T. Nakajima, Y. Honda, O. Kitao, H. Nakai, M. Klene, X. Li, J. E. Knox, H. P. Hratchian, J. B. Cross, V. Bakken, C. Adamo, J. Jaramillo, R. Gomperts, R. E. Stratmann, O. Yazyev, A. J. Austin, R. Cammi, C. Pomelli, J. W. Ochterski, P. Y. Ayala, K. Morokuma, G. A. Voth, P. Salvador,

 This journal is © The Royal Society of Chemistry 2018

Open Access Article. Published on 14 May 2018. Downloaded on 1/20/2026 1:24:30 PM.
This article is licensed under a Creative Commons Attribution-NonCommercial 3.0 Unported Licence.

J. J. Dannenberg, V. G. Zakrzewski, S. Dapprich, A. D. Daniels, M. C. Strain, O. Farkas, D. K. Malick, A. D. Rabuck, K. Raghavachari, J. B. Foresman, J. V. Ortiz, Q. Cui, A. G. Baboul, S. Clifford, J. Cioslowski, B. B. Stefanov, G. Liu, A. Liashenko, P. Piskorz, I. Komaromi, R. L. Martin, D. J. Fox, T. Keith, A. Laham, C. Y. Peng, A. Nanayakkara, M. Challacombe, P. M. W. Gill, B. Johnson, W. Chen, M. W. Wong, C. Gonzalez and J. A. Pople, *Gaussian 09, Rev. E.01*, Gaussian, Inc., Wallingford, CT, 2009.